Journal of Experimental Botany, Vol. 77, No. 2 pp. 445–462, 2026
https://doi.org/10.1093/jxb/eraf364 Advance Access Publication 23 August 2025

RESEARCH PAPER

Wood-specific modification of glucuronoxylan can enhance growth in *Populus*

János Urbancsok[1], Evgeniy N. Donev[1,2], Marta Derba-Maceluch[1], Pramod Sivan[1,3], Félix R. Barbut[1], Madhusree Mitra[1], Zakiya Yassin[4], Kateřina Cermanová[5], Jan Šimura[1], Michal Karady[5], Gerhard Scheepers[4], and Ewa J. Mellerowicz[1,*]

[1] Department of Forest Genetics and Plant Physiology, Umeå Plant Science Centre, Swedish University of Agricultural Sciences, Umeå 901 83, Sweden
[2] Center of Plant Systems Biology and Biotechnology, 14 St. Knyaz Boris I - Pokrastitel str., Plovdiv 4023, Bulgaria
[3] Division of Glycoscience, Department of Chemistry, KTH Royal Institute of Technology, AlbaNova University Centre, Stockholm 106 91, Sweden
[4] RISE Research Institutes of Sweden, Drottning Kristinas väg 61, Stockholm 11428, Sweden
[5] Laboratory of Growth Regulators, Institute of Experimental Botany, the Czech Academy of Sciences & Palacký University, Šlechtitelů 27, Olomouc CZ-779 00, Czech Republic

* Correspondence: ewa.mellerowicz@slu.se

Received 31 March 2025; Accepted 11 August 2025

Editor: Mary Byrne, University of Sydney, Australia

Abstract

Xylem cells are surrounded by primary and secondary cell walls. Formation of primary walls is regulated by the cell wall integrity surveillance system, but it is unclear if the deposition of secondary walls is similarly regulated. To study this question, we introduced to aspen three different enzymes cleaving cell wall-localized xylan and we suppressed xylan synthase components either ubiquitously or specifically during secondary wall formation using the *Populus trichocarpa GT43B* promoter. When xylan was ubiquitously altered, 95% of lines showed reduced growth, whereas when it was altered during secondary wall deposition, 30% of lines grew better, with the rest having no growth impairment, suggesting opposite effects of primary and secondary wall disturbances. To detect the mechanism of growth stimulation by disturbed deposition of the secondary wall, we analyzed changes in wood quality traits, chemistry, transcriptomics, metabolomics and hormonomics in transgenic lines. We found increased tension wood production, reduced S- and H-lignin, and changes in several metabolites in common in these lines. Remorin *REM1.3* and *NRL2* (*NPH3* family) transcripts increased, and changes in jasmonates, abscisic acid, and salicylic acid occurred in secondary wall-forming xylem, suggesting their involvement in secondary wall integrity surveyance and signaling. The data indicate that a unique program mediates responses to secondary wall impairment that induces growth.

Keywords: Aspen, cell wall integrity sensing, glucuronoxylan, secondary cell wall, secondary cell wall integrity, transgenic *Populus* trees, wood development.

Introduction

The plant cell wall has many essential functions such as protecting protoplasts from abiotic and biotic stresses, regulating cell growth, generating cell shape, providing means for regulation of cellular adhesion, and offering the medium for water and nutrient transport in different tissues. Therefore, cell wall status is expected to be tightly monitored.

Plant cell wall monitoring systems using chemical and mechanical cues have been reported in different types of growing cells (Vaahtera *et al.*, 2019). The best-established mechanism of cell wall status surveillance operates via plasma membrane-located receptor-like kinases from the *Catharanthus roseus* receptor-like kinase 1-like family (*Cr*RLK1L) such as THESEUS1 (THE1) and FERONIA (FER). These receptors form signaling complexes interacting among themselves and with other proteins including glycosylphosphatidylinositol (GPI)-anchored co-receptors or LEUCINE-RICH REPEAT EXTENSINs (LRXs) (Doblas *et al.*, 2018). They are thought to perceive wall damage by their extracellular domains interacting with de-methylesterified pectin and anionic peptides called rapid alkalinization factors (RALFs), and to transduce the signals via phosphorylation relay cascades and G-protein-mediated signaling, triggering changes in Ca^{2+} fluxes, production of reactive oxygen species (ROS) in the apoplast, and apoplast alkalinization. In the growing pollen tubes and root hairs, the integrity of the cell wall is directly monitored in the apoplast by RALFs, which bind with high affinity to LRXs and de-esterified pectin and with low affinity to *Cr*RLK1L–GPI–protein signaling complexes, providing a means for monitoring LRX–homogalacturonan status in the cell wall (Moussu *et al.*, 2023; Schoenaers *et al.*, 2024). Another well-studied group of proteins perceiving signals from the cell wall are different types of wall-associated kinases (WAKs) which are thought to monitor the pectin status in the cell wall by interacting with homogalacturonan and its fragments having specific methylesterification status, and then transducing the signal to the kinase domain in the cytoplasm (Kohorn, 2016). Rice WAK11 was shown to regulate the diurnal pattern of growth by controlling the activity of brassinosteriod receptor BRI1 in a pectin methylesterification-dependent manner (Yue *et al.*, 2022). Many other chemical signals such as cell wall fragments, peptides, or extracellular ATP are generated during growth and pathogen attack. These signals are known as damage-associated molecular patterns (DAMPs), and their perception via various pattern recognition receptors has been described in pathways related to cell wall integrity and pathogen sensing, which are overlapping and regulate each other (Engelsdorf *et al.*, 2018). The perception of mechanical signals during cell wall integrity stress is less well understood, but it is likely to involve stretch-activated channels such as Ca^{2+}-influx MID1-COMPLEMENTING ACTIVITY 1 (MCA1) and REDUCED HYPEROSMOLALITY-INDUCED [Ca^{2+}] INCREASE 1 (OSCA1) located in the plasma membrane, which sense low and high osmotic stress, respectively, in the apoplast and activate Ca^{2+}-dependent and abscisic acid (ABA) signaling (Vaahtera *et al.*, 2019). Thus, mechanical signaling during cell wall integrity sensing is expected to interact with abiotic stress perception mediated by ABA, such as drought, osmotic, or freezing stress.

Much less is known about perception of cell wall integrity in non-growing cells such as secondary cell wall-depositing xylem cells. The evidence for such a signaling mechanism includes: (i) activation of immune responses and biotic resistance when the secondary cell wall is specifically affected (Hernández-Blanco *et al.*, 2007; Gallego-Giraldo *et al.*, 2011a; Pogorelko *et al.*, 2013; Pawar *et al.*, 2016; Molina *et al.*, 2021); (ii) activation of abiotic stress responses and increased abiotic stress resistance when secondary walls are affected (Chen *et al.*, 2005; Ramírez and Pauly, 2019; Barbut *et al.*, 2024); (iii) stimulation of growth or induction of developmental changes in primary-walled cells by alterations of secondary walls (Bosca *et al.*, 2006; Biswal *et al.*, 2015; Derba-Maceluch *et al.*, 2015; Ratke *et al.*, 2018); (iv) induction of immune responses (Mélida *et al.*, 2020; Dewangan *et al.*, 2023) or developmental changes (Kákošová *et al.*, 2013; Zhao *et al.*, 2013) by secondary wall-derived oligosaccharides; and (v) recovery of growth defects of secondary wall mutants displaying dwarfism by eliminating certain signaling/regulatory proteins and hormones (Gallego-Giraldo *et al.*, 2011b; Bonawitz *et al.*, 2014; Ramírez *et al.*, 2018; Ramírez and Pauly, 2019).

In the case of lignin mutants that are dwarf, the mechanism of immune responses has been partly elucidated. It involves FER signaling that induces ARABIDOPSIS DEHISCENCE ZONE POLYGALACTURONASE 1 (ADPG1) and ADPG1-mediated release of oligogalacturonides that activate immune defenses in a WAK-dependent way (Gallego-Giraldo *et al.*, 2020; Liu *et al.*, 2023). Given the reports of secondary wall xylan modifications leading to increased growth (Biswal *et al.*, 2015; Derba-Maceluch *et al.*, 2015; Ratke *et al.*, 2018), we aimed to investigate mechanisms potentially responsible for this effect. Therefore, we induced different types of xylan alterations in secondary cell walls in aspen and classified them according to their effect on growth. We subsequently selected those transgenic modifications that resulted in growth stimulation and characterized the changes in cell walls, metabolomes, hormonomes, and transcriptomes of wood-forming tissues at both the primary and secondary wall stages in the transgenic plants. We detected some common reactions in these plants that could be part of a shared response linking secondary wall defects with increased growth.

Materials and methods

Transgenic lines and wild type

Hybrid aspen (*Populus tremula* L. × *tremuloides* Michx.), clone T89, was used as a wild type. Transgenic lines expressing different fungal

xylan-active enzymes (Table 1) were generated using *Agrobacterium*-mediated transformation and vectors described in previous publications (Latha Gandla *et al.*, 2015; Donev *et al.*, 2025; Derba-Maceluch *et al.*, 2023; Barbut *et al.*, 2024; Sivan *et al.*, 2025). Lines with the highest transgene expression or native gene suppression were selected from at least 20 independent lines per construct. Lines with suppressed native xylan biosynthetic *GT43* genes were selected among the lines described in an earlier publication (Ratke *et al.*, 2018).

Greenhouse conditions, growth analyses, and tissue collection

In vitro propagated saplings were planted in soil, and grown for 9 weeks in the phenotyping platform (WIWAM Conveyor, custom designed by SMO, Eeklo, Belgium) as described by Wang *et al.* (2022) and Urbancsok *et al.* (2023). Briefly, the conditions were 18 h/6 h (day/night) with light having 160–230 μmol m^{-2} s^{-1} intensity during the day provided by white light (FL300 LED Sunlight v1.1) and far-red light (FL100 LED custom-made, 725–735 nm) from Senmatic A/S (Søndersø, Denmark), 22 °C/18 °C temperature, and an average air relative humidity of 60%. Plants were watered automatically based on weight, and their height was automatically measured.

At harvest, the trees were photographed, and their stem diameters (at the base) and above-ground FWs were recorded. For RNA, hormonomics, and metabolomics analyses, a 30 cm long stem segment above internode 37 was dissected, debarked, frozen in liquid nitrogen, and stored at −70 °C. Frozen bark and frozen wood core were scraped with a scalpel into a pre-cooled mortar and ground in liquid nitrogen to obtain frozen cambium/phloem and developing xylem powder, respectively.

The stem below internode 37 was used for determining average internode length. For SilviScan analysis, the 4 cm long segment from the base of the stem was used, and the remaining stem was debarked and freeze-dried for 48 h for wood chemistry analyses. Below-ground biomass was determined by weighing cleaned and air-dried roots.

Reverse transcription–PCR

To isolate total RNA, frozen cambium/phloem and xylem powders (~100 mg) were extracted with cetyltrimethylammonium bromide (CTAB)/chloroform:isoamylalcohol (24:1), followed by precipitation with LiCl and sodium acetate/ethanol (Chang *et al.*, 1993). Reverse transcription–PCR (RT–PCR) procedures followed the protocol described by Sivan *et al.* (2025). UBQ-L (Potri.005G198700) and ACT11 (Potri.006G192700) were selected as reference genes. The primer sequences are listed in Supplementary Table S1. The relative expression level was calculated according to Pfaffl (2001).

SilviScan and near infrared analysis

Wood quality traits were analyzed using a SilviScan instrument (RISE, Stockholm, Sweden) as described by Urbancsok *et al.* (2023) for six transgenic trees per line and 12 wild-type trees. The same samples were scanned by a near infrared (NIR; 960–2500 nm at 256 wavelengths) scanner at 30 μm resolution, and tension wood was predicted for each pixel using a procedure described by Renström *et al.* (2025). Heatmaps showing tension wood distributions were subsequently produced and the average probability of tension wood was calculated for each sample.

Cell wall chemical analyses

Wood was analyzed in three trees per line, as described by Sivan *et al.* (2025). Briefly, the wood powder was obtained by filing the freeze-dried wood and sieving the sawdust with a Retsch AS 200 analytical sieve shaker (Retsch GmbH, Haan, Germany) to a particle size between 50 μm and 100 μm. Approximately 50 μg (±10 μg) of this powder was used in a pyrolizer (PY-2020iD and AS-1020E, Frontier Lab, Japan) connected to a GC/MS (7890A/5975C, Agilent Technologies Inc., Santa Clara, CA, USA) to analyze main wood components including carbohydrates, H-, G-, and S-lignin units, and phenolic compounds, as described by Gerber *et al.* (2012). The composition of matrix polysaccharides was analyzed using the methanolysis–trimethylsilyl (TMS) procedure as described by Pramod *et al.* (2021). Briefly, the alcohol-insoluble residue (AIR) prepared according to Latha Gandla *et al.* (2015) was destarched by α-amylase (from pig pancreas, cat. no. 10102814001, Roche, USA) and amyloglucosidase (from *Aspergillus niger* cat. no.10102857001, Roche) enzymes, and used to prepare silylated monosaccharides that were separated by GC-MS (7890A/5975C; Agilent Technologies Inc.) as described in Latha Gandla *et al.* (2015). Raw data MS files from GC-MS analysis were converted to CDF format in Agilent Chemstation Data Analysis (v.E.02.00.493) and exported to R software (v.3.0.2). 4-*O*-methylglucuronic acid (meGlcA) was identified according to Chong *et al.* (2013).

Hormonomics

Frozen cambium/phloem and developing xylem tissue powders were extracted and subjected to GC-MS analysis as described by Šimura *et al.* (2018), with slight modifications (Urbancsok *et al.*, 2023). The immediate non-volatile precursor of the plant hormone ethylene, 1-aminocyclopropane-1-carboxylic acid (ACC), was measured using LC-MS/MS, following the methodology in Karady *et al.* (2024). All identified hormones including their precursors and inactivated forms are listed in Supplementary Table S2.

Metabolomics

Metabolic profiling was performed by GC-MS and LC-MS at the Swedish Metabolomics Centre, Umeå, Sweden as described previously (Gullberg *et al.*, 2004). Approximately 10 mg of cambium/phloem and developing xylem tissue was extracted using an extraction buffer (20:20:60, chloroform:water:methanol, v/v/v) with internal standards. For LC-MS, the samples were analyzed using an Agilent 1290 Infinity UHPLC system (Agilent Technologies, Waldbronn, Germany) coupled to a 6546 Q-TOF mass spectrometer (Agilent Technologies Inc.), with chromatographic and mass spectrometric parameters optimized for both positive and negative ion modes. GC-MS analysis involved derivatized samples analyzed on an Agilent 7890B gas chromatograph (Restek Corporation, Bellefonte, PA, USA) coupled to a Pegasus BT TOF-MS (Leco Corp., St Joseph, MI, USA), with detailed instrumental settings and data processing performed using ChromaTOF, MATLAB (Mathworks, Natick, MA, USA), and NIST MS 2.2 software (https://chemdata.nist.gov/mass-spc/ms-search/downloads/).

Data processing for LC-MS included targeted feature extraction using in-house libraries, while GC-MS employed retention index and mass spectral comparisons for metabolite identification as described in Schauer *et al.* (2005). Further technical details, including specific instrument settings and data processing methodologies, are provided in the Supplementary Protocol S1.

Transcriptomics

For transcriptomics, RNA from five trees per transgenic line and eight trees from the wild type was purified as described by Urbancsok *et al.* (2023) and used for cDNA preparation and sequencing at Novogene Co., Ltd (Cambridge, UK). Quality control and mapping to the *Populus tremula* transcriptome (v.2.2), retrieved from the PlantGenIE (https://plantgenie.org; Sundell *et al.*, 2015), and to sequences used in fungal vectors were carried out by Novogene. Raw counts were used for differential expression analysis in R (v.3.4.0) employing the Bioconductor (v.3.4) DESeq2 package (v.1.16.1), as described by

Table 1. List of constructs used in this study

Construct	Gene ID	Organism	Function	Reference
35S:GH67	GenBank: DR701927.1	*Aspergillus niger*	Ubiquitous overexpression of α-glucuronidase from family GH67 reducing xylan glucuronidation	Derba-Maceluch *et al.* (2023)
WP:GH67			Secondary wall-specific overexpression of α-glucuronidase from family GH67 reducing xylan glucuronidation in secondary walls	
35S:GH10	GenBank: ABF50851.1	*Aspergillus nidulans*	Ubiquitous overexpression of endo-β-1,4-xylanase from family GH10 reducing xylan backbone	Barbut *et al.* (2024); Sivan *et al.* (2025)
WP:GH10			Secondary wall-specific overexpression of endo-β-1,4-xylanase from family GH10 reducing xylan backbone in secondary walls	
35S:GH11	GenBank: XP_661217.1		Ubiquitous overexpression of endo-β-1,4-xylanase from family GH11 reducing xylan backbone	
WP:GH11			Secondary wall-specific overexpression of endo-β-1,4-xylanase from family GH11 reducing xylan backbone in secondary walls	
35S:*Pc*GCE	GenBank: JQ972915.1	*Phanerochaete carnosa*	Ubiquitous overexpression of glucuronoyl esterase from family CE15 reducing xylan ester linkages to lignin	Latha Gandla *et al.* (2015); Donev *et al.* (2025)
WP:*Pc*GCE			Secondary wall-specific overexpression of glucuronoyl esterase from family CE15 reducing xylan ester linkages to lignin in secondary walls	
35S: GT43-rnai	Potri.002G107300/Potra2n2c5445-*Pt*GT43E Potri.007G047500/Potra2n7c16228-*Pt*GT43C	*Populus tremula* x *tremuloides*	Ubiquitous suppression of IRX9L and IRX14 proteins, that make part of primary wall xylan synthase complex, by RNAi	Ratke *et al.* (2018)
WP: GT43-rnai	Potri.016G086400/Potra2n16c30051-*Pt*GT43B Potri.007G047500/Potra2n7c16228-*Pt*GT43C		Secondary wall-specific suppression of IRX9 and IRX14 proteins, that make part of secondary wall xylan synthase complex, by RNAi	

Kumar *et al.* (2019). The best BLAST hits were identified in *Populus trichocarpa* (v.3.1) and *Arabidopsis thaliana* (v.11.0).

A weighted gene correlation network analysis (WGCNA) was obtained using the R [v.3.4.0; https://www.R-project.org] library WGCNA (Langfelder and Horvath, 2008). Gene modules were correlated with traits from growth, hormonomics, metabolomics, and SilviScan data. Genes from selected modules were used to design co-expression gene networks obtained using PlantGenIE tools. The networks were visualized by Cytoscape (v.3.6.0) (Shannon *et al.*, 2003).

Statistical analyses

Unless otherwise stated, univariate statistical analyses were performed in JMP Pro (v.16.0) software (SAS Institute Inc., Cary, NC, USA).

Results

Growth of transgenic lines with modified xylan

To investigate which types of xylan modification increase growth, we used 43 transgenic hybrid aspen lines carrying 10 different constructs that were designed to induce different types of xylan modifications (Table 1). The majority of these lines were expressing different fungal enzymes acting on xylan and targeted to cell walls using previously described strategies (Derba-Maceluch *et al.*, 2023; Barbut *et al.*, 2024; Sivan *et al.*, 2025). The enzymes included a xylan α-glucuronidase from family GH67, two endo-β-1,4-xylanases from families GH10 and GH11, and a glucuronoyl esterase from family CE15. In other lines, different members of the xylan synthase complex from family GT43 were suppressed (Ratke *et al.*, 2018). The transgenes were expressed by either a ubiquitous (35S) promoter or the wood-specific promoter (WP). The WP was isolated from the *P. trichocarpa GT43B* gene and was found to be active during secondary wall biosynthesis (Ratke *et al.*, 2015). In the case of native *GT43* genes, the 35S construct targeted the primary wall xylan synthase genes *PtGT43C* and *PtGT43E*, whereas the WP construct affected expression of the secondary wall xylan synthase genes *PtGT43B* and *PtGT43C* (Ratke *et al.*, 2018).

The modification of xylan differentially affected growth, depending on the kind of transgene, the type of promoter, and

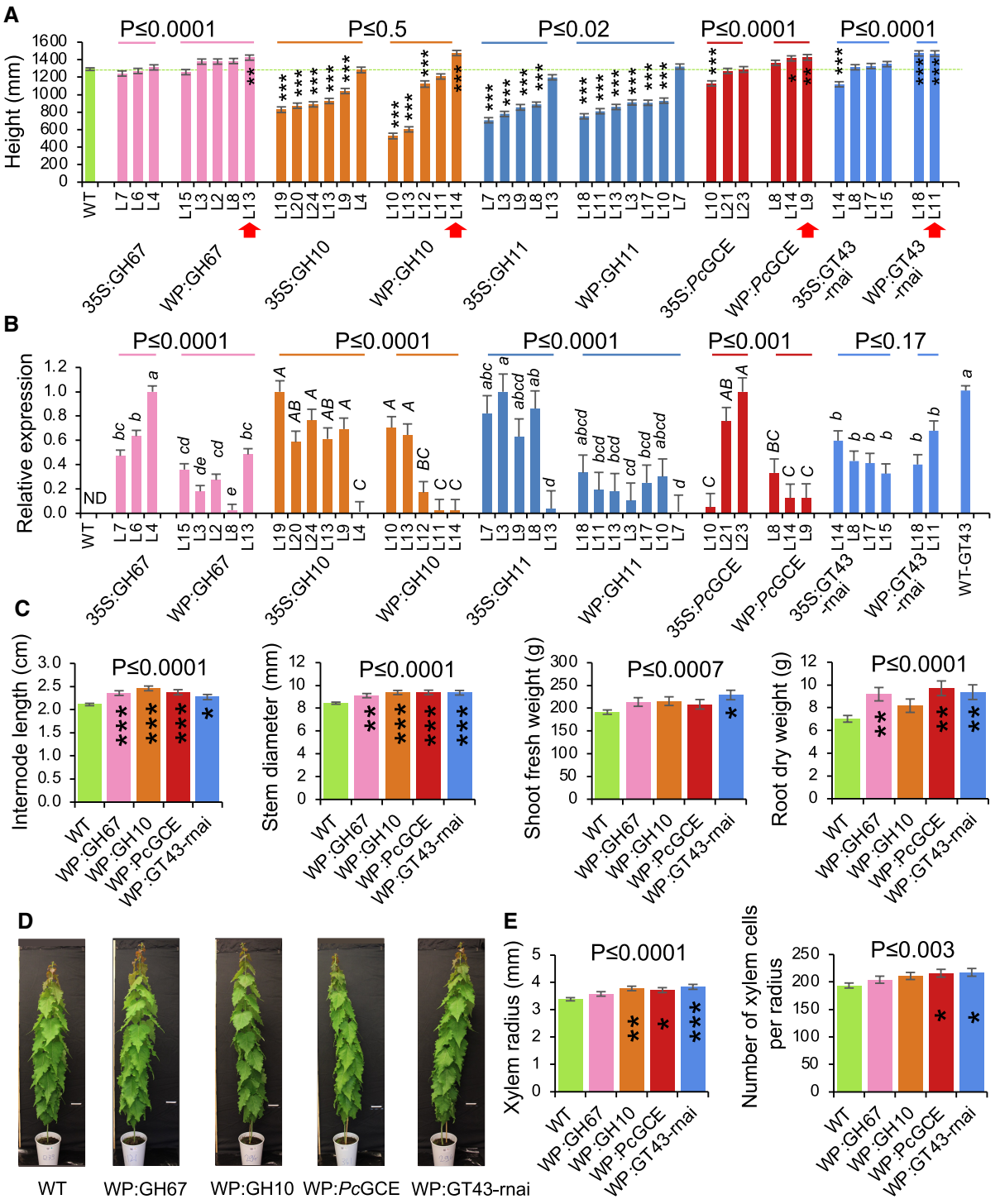

Fig. 1. Xylan modification affects growth of hybrid aspen. (A) Height of transgenic lines with modified xylan either ectopically (35S) or specifically in secondary walls (WP). Red arrows indicate lines with increased growth selected for further analysis. (B) Relative expression levels of transgenes in lines overexpressing fungal enzymes (GH67, GH10, GH11, and *Pc*GCE) or targeted native *PtGT43C* normalized to the highest expressing line. ND, transgenes were not detected in wild-type (WT) samples. For each transgene/gene, the means accompanied by the same letter are not significantly different ($P \leq 0.05$, Tukey's test). (C) Different morphological parameters of selected lines with increased growth. (D) Representative individuals of selected lines. (E) Xylem production determined by SilviScan analysis of wood in selected lines. Data are means ± SE; $n = 6$, 3, or 6 trees for transgenic lines and $n = 24$, 6, or 12 trees for the WT in (A, C), (B), or (E), respectively. $^{*}P \leq 0.05$; $^{**}P \leq 0.01$; $^{***}P \leq 0.001$ for comparisons with the WT by Dunnett's test. *P*-values above the bars show significance of differences between 35S and WP promoters (A, B) or between the WT and all selected lines (C, E) (post-ANOVA contrast). The height data for some lines expressing xylanases have been reported by Sivan *et al*. (2025) and are shown here for comparative purposes.

the level of transgene expression (Fig. 1A, B). The *GH67* transgene induced growth when highly expressed specifically in the secondary walled tissues, but not when the 35S promoter was used. The transgene expression level was similar or higher in 35S promoter-driven lines compared with those driven by the WP. Endo-β-1,4-xylanases (GH10 and GH11) by and large inhibited growth regardless of the promoter, and their effect was proportional to transgene expression. The exception was a low-expressing GH10 line with WP, which had significantly increased height compared with the wild type. Glucuronoyl esterase-expressing lines exhibited premature senescence when the 35S promoter was used, as was previously observed (Latha Gandla *et al.*, 2015; Donev *et al.*, 2025), and their height was affected in one of the studied lines. Interestingly, the same transgene driven by WP showed growth stimulation (Fig. 1A). In this case, the phenotype was dependent on the choice of promoter rather than the transgene expression level. The suppression of primary wall xylan synthase complex members, *Pt*GT43C and *Pt*GT43E, using 35S promoter RNAi constructs, resulted in growth inhibition or no effect, but the suppression of the secondary wall xylan synthase complex members, *Pt*GT43B and *Pt*GT43C, using WP led to enhanced growth, as previously observed (Ratke *et al.*, 2018). In summary, for four out of five transgenes there was a significant difference between promoters, with better growth when WP was used, and all the best performing individual lines had WP-driven transgenes. For all four fungal genes studied here, the expression levels were lower when WP was used compared with the 35S promoter, whereas *PtGT43C* native gene suppression was not affected by the promoter. Thus, the data support the hypothesis that xylan modification induced specifically in secondary walls can increase growth, but this is conditional on the transgene type and its expression level.

Four transgenic lines with different types of transgenes all exhibiting increased stem height were subsequently selected for thorough phenotypic analyses. The selected individual lines had increased internode length and stem diameter, and collectively they had greater shoot FW and root DW than the wild type but showed no alterations in general morphology (Fig. 1C, D). Wood quality traits analyzed by SilviScan showed no effect of genotype on any of the analyzed parameters, indicating that wood anatomy and physical properties did not differ in xylan-modified lines with increased growth from the wild type (Supplementary Table S3). However, there was an increase in xylem radius and number of xylem cells per radius in three or two lines, respectively, and when comparing all transgenic lines combined with wild-type plants, indicating increased xylem production by the cambium in transgenic lines with increased height growth (Fig. 1E).

As young aspen trees typically form some tension wood even when growing upright, we wondered if tension wood formation was affected in transgenic lines with modified secondary wall xylan and increased growth. To test this, we used NIR spectroscopy of the cut stem surface at the base of the stems that allows us to accurately predict the occurrence of tension wood based on cell wall chemical fingerprints (Renström *et al.*, 2025). The heatmaps showing the distribution of probability of tension wood and its quantification indicated a greater occurrence of this tissue in the transgenic lines compared with the wild type (Fig. 2).

Wood cell wall composition analyses in xylan-modified lines with increased growth show slightly reduced lignification

The transgenic modifications of selected lines were targeted to developing secondary walls, hence we analyzed their wood cell wall composition. Matrix polysaccharides were only slightly affected in the GH67-overexpressing line that exhibited an increase in mannose and reductions in meGlcA (expected based on the GH67 enzyme activity) and galacturonic acid (GalA) (Fig. 3A). GH10 induced increases in mannose and pectin-related sugars: arabinose, rhamnose, and GalA. *Pc*GCE induced increased glucuronic acid, and suppression of endogenous *GT43B* and *GT43C* genes resulted in a small decrease in xylose as observed before (Ratke *et al.*, 2018). Overall, these changes were small and specific for each transgene.

Despite the transgenes targeting secondary wall xylan in different ways, some common changes in cell wall were revealed by pyrolysis–GC/MS analysis. The overall carbohydrate content of the transgenic lines seemed to be greater than in the wild type, which was at the expense of lignin especially the S- and H-lignin units (Fig. 3B). In contrast, the G-lignin content increased in the *PtGT43*-suppressed line but decreased in GH67- and GH10-expressing lines, resulting in variable trends in the S-/G-lignin ratio among the lines.

Hormonomics analyses in transgenic lines with increased growth indicate changes in cytokinins, jasmonates, abscisic acid, and salicylic acid

To investigate if different types of xylan modification in secondary walls affected similar hormonal pathways, we carried out hormonomics analyses (Šimura *et al.*, 2018) detecting different forms of cytokinins, auxins, jasmonates, salicylic acid (SA), ABA, and ACC (Supplementary Table S2). Separate cambium/phloem samples including cells with primary walls, and developing xylem samples containing cells depositing secondary walls were analyzed. Among the cytokinins, the cytokinin precursor *cis*-zeatin riboside (*c*ZR), which was the most abundant species, increased in two or three out of four tested lines in the cambium/phloem and xylem tissues, respectively, with a similar tendency detected for all analyzed lines in both tissues (Fig. 4). Indole-3-acetic acid (IAA) and its oxidation product oxIAA had a tendency to decrease in the cambium/phloem. The precursor of jasmonic acid (JA), *cis*-12-oxophytodienoic acid (*cis*-OPDA), decreased significantly in two transgenic lines in the xylem, with a similar pattern observed for all lines in both

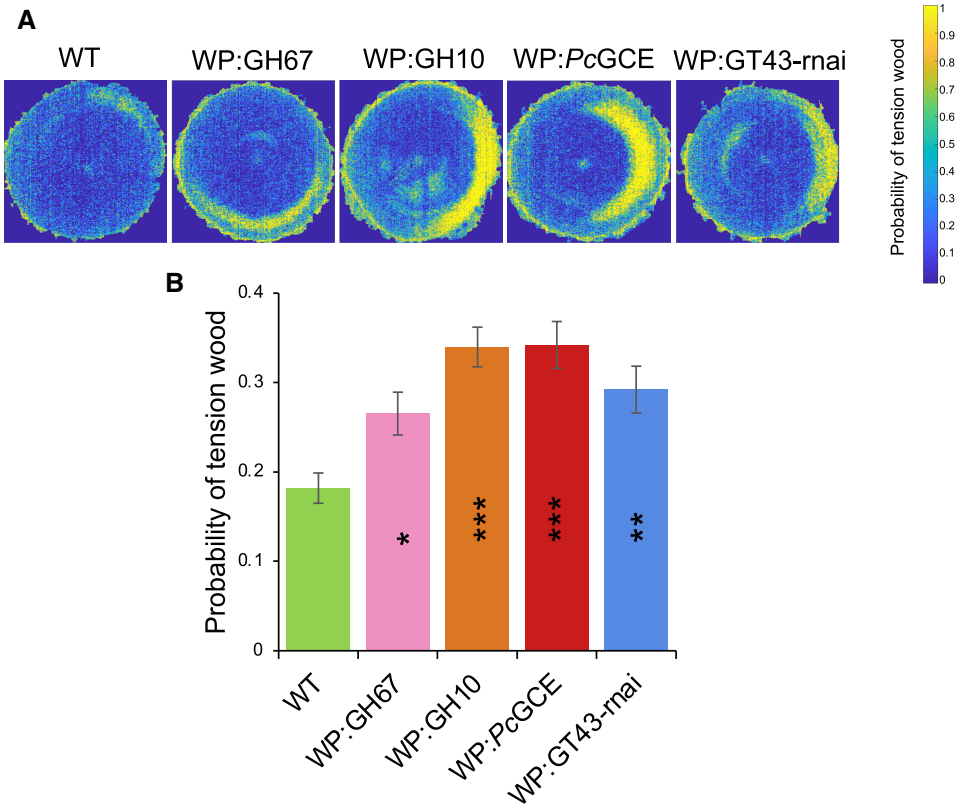

Fig. 2. Transgenic lines with xylan defects in secondary walls and increased growth produce more tension wood compared with the wild type (WT). (A) Tension wood probability shown as heatmaps of representative NIR images for transgenic lines and the WT. (B) Quantification of tension wood probability. Data are means ± SE; $n = 6$ trees for transgenic lines and $n = 12$ trees for the WT. $^{*}P \leq 0.05$; $^{**}P \leq 0.01$; $^{***}P \leq 0.001$ for comparisons with the WT by Dunnett's test.

analyzed tissues, whereas its downstream reaction product JA showed some tendency to increase, but the levels of JA were very variable among individual plants, resulting in high probability values. SA decreased significantly in two transgenic lines in the xylem, and all lines showed a similar tendency in both tissues. ABA contents tended to be reduced in the cambium/phloem of transgenic lines compared with the wild type, whereas the changes were negligible in the developing xylem tissue. ACC was affected only in the line WP:*Pc*GCE that had higher levels of this precursor than the wild type in the xylem (Supplementary Table S2). To conclude, the common changes in different xylan-modified lines compared with the wild type included elevated *c*ZR contents in both tissues, decreased IAA and oxIAA amounts in the cambium/phloem, reduced levels of *cis*OPDA in both tissues, probably due to the biosynthesis of JA, as well as reduced contents of ABA in the cambium/phloem and SA in both tissues.

Xylan-modified lines with better growth performance exhibited common changes in metabolites

To further investigate whether different types of xylan modification in secondary walls resulting in better growth affected similar metabolic pathways or not, we carried out metabolomics analyses using both GC and LC. Among the 300 metabolites identified by these analyses in the wood-forming tissues (cambium/phloem and developing xylem), 64 were affected in transgenic samples specifically in the cambium/phloem tissues, 21 were affected only in the developing xylem, and 20 were affected in both tissues when compared with the wild type (Fig. 5A). The metabolites were classified (Supplementary Table S4) and the affected groups are shown as volcano plots (Fig. 5B). In the cambium/phloem tissues, there was a decreased abundance in amino acids and increased phenolic glycosides. Some lignols and other phenylpropanoids were also slightly increased in both tissues. There were decreased levels of phenylalanine that serves as the phenylpropanoid precursor, and of threonine and methionine. They were altered in the cambium/phloem only, whereas methionine was reduced in both tissues. In addition, some monosaccharides increased in abundance in the transgenic lines, including xylose, arabinose, and arabitol in both tissues; xylobiose and a related xylitol also increased in the cambium/phloem tissues. The observed metabolic alterations point towards common changes in the phenylpropanoid pathway in xylan-impaired lines that led to higher levels of phenolic

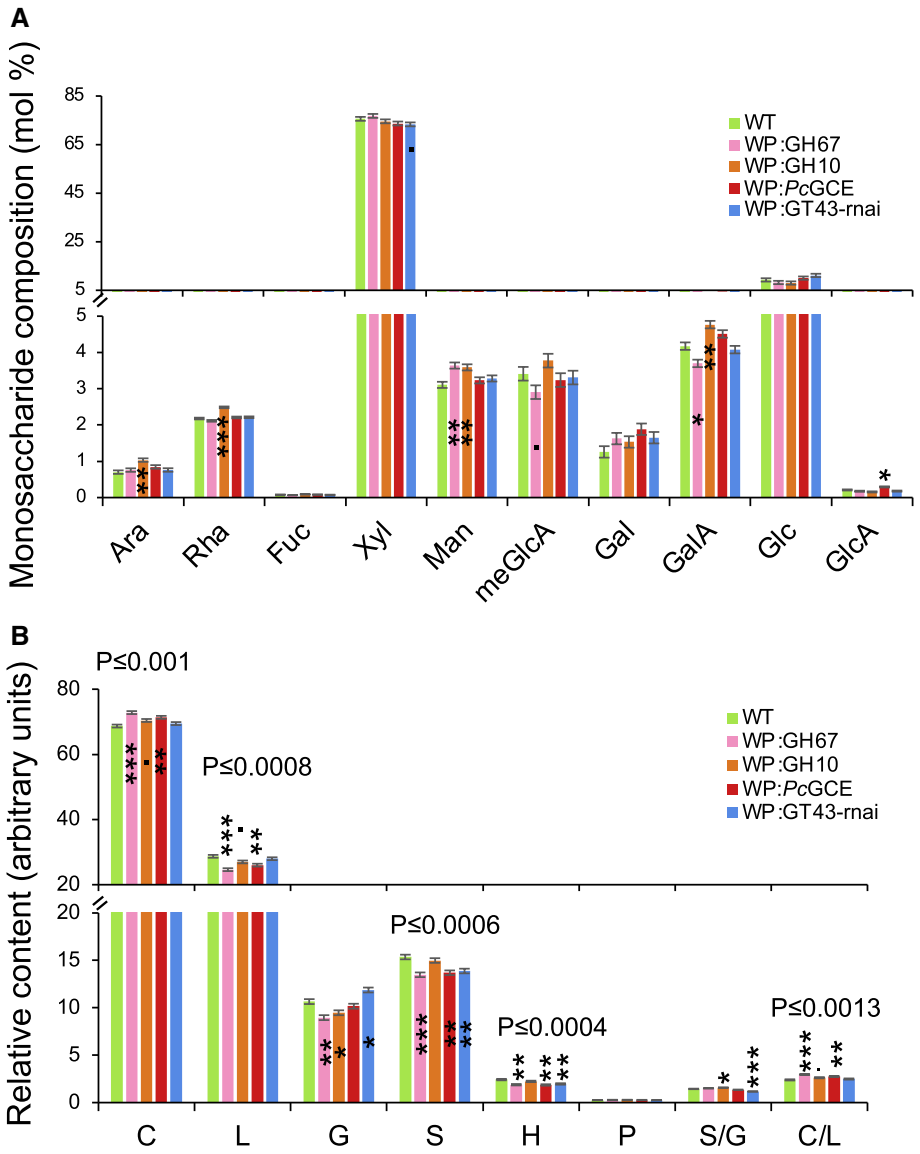

Fig. 3. Changes in wood cell wall composition in xylan-modified lines with increased growth. (A) Monosaccharide composition of matrix polysaccharides analyzed by methanolysis–trimethylsilyl analysis. (B) Cell wall composition according to pyrolysis–GC-MS. Data are means ± SE; $n = 3$. Significant differences for individual lines compared with the wild type (WT) according to Dunnett's test are indicated as follows: ·$P \leq 0.1$; -$P \leq 0.05$; *$P \leq 0.05$; **$P \leq 0.01$; ***$P \leq 0.001$. *P*-values above the bars in (B) show the significance of differences between the WT and all lines collectively (post-ANOVA contrast). Ara, arabinose; Fuc, fucose; Gal, galactose; GalA, galacturonic acid; Glc, glucose; GlcA, glucuronic acid; Man, mannose; meGlcA, 4-*O*-methylglucuronic acid; Rha, rhamnose; Xyl, xylose. C, carbohydrates; G, guaiacyl lignin units; H, *para*-hydroxyphenyl lignin units; L, total lignin (S + G + H); P, phenolics; S, syringyl lignin units.

glycosides, and xylan-related sugars. Last, but not least, the metabolomics analysis confirmed the reduced SA level in the xylem (Supplementary Table S4).

Commonly affected transcripts detected in transgenic lines with better growth

To reveal if the different xylan modifications in the transgenic lines with enhanced growth induced common transcriptomic changes, RNA sequencing was performed in the cambium/phloem and developing xylem tissues.

In the cambium/phloem of transgenic xylan-modified lines, between six and 136 genes were differentially expressed compared with the wild type [$P_{adj} \leq 0.01$, $|\log_2(\text{fold change})| \geq 0.584$], and no commonly affected genes were observed (Fig. 6; Supplementary Table S5). In contrast, in developing xylem, between 17 and 128 genes were differentially expressed, and three genes were affected in common in all the lines. One of them has no assigned function and no homologs in other species except poplars. The second gene is similar to Arabidopsis *NRL2* from the *NPH3* family of plant-specific adapter protein genes and the third one is similar to

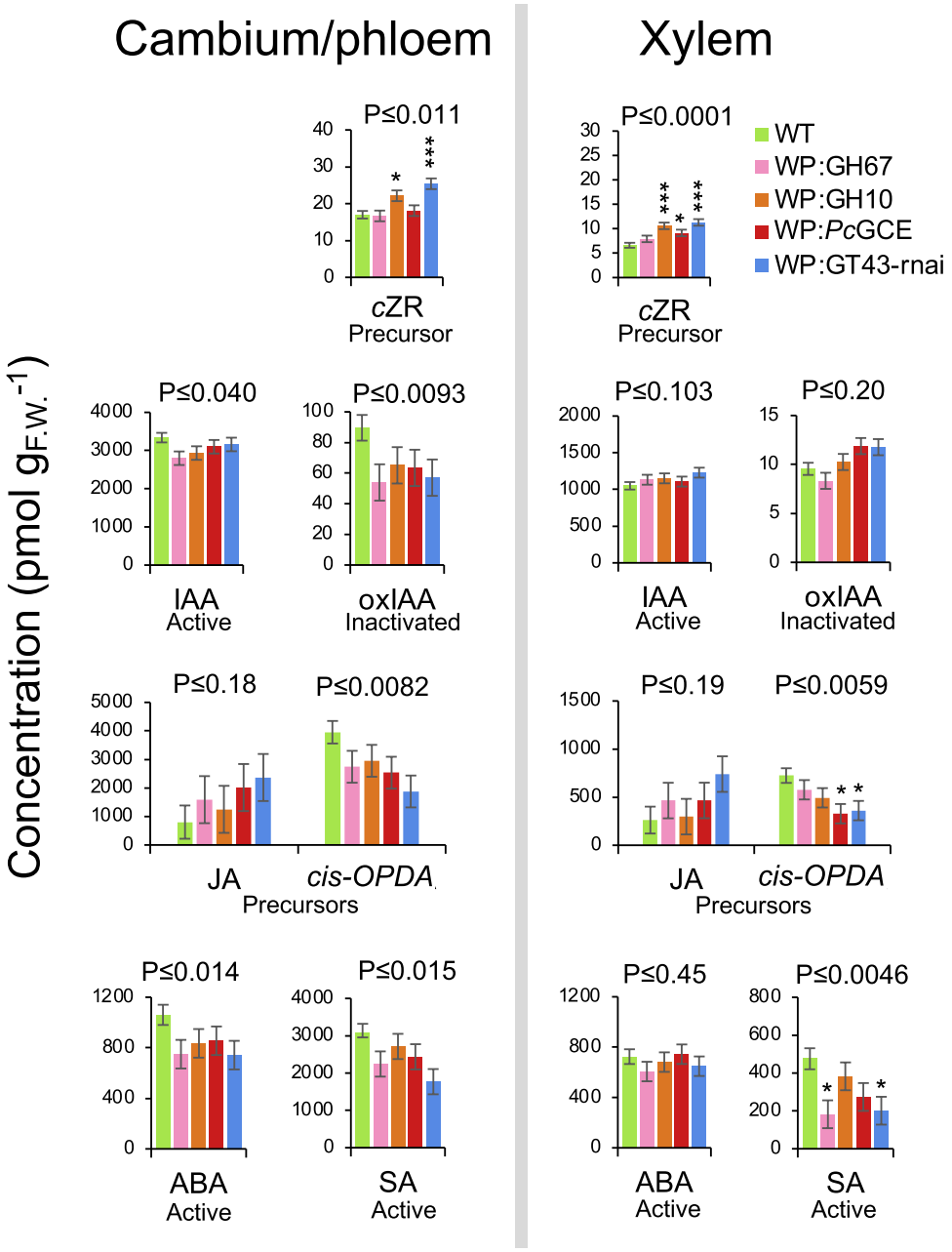

Fig. 4. Changes in hormonal status in wood-forming tissues of xylan-modified lines with increased growth. Data are means ± SE; n= 4 for transgenic lines and n=8 for the wild type (WT). Asterisks indicate the significance of differences compared with the WT by Dunnett's test: $^{*}P \leq 0.05$; $^{**}P \leq 0.01$; $^{***}P \leq 0.001$. P-values above the bars show the significance of differences between the WT and all lines (post-ANOVA contrast). ABA, abscisic acid; *cis*-OPDA, *cis*-12-oxophytodienoic acid; cZR, *cis*-zeatin riboside; IAA, indole-3-acetic acid; JA, jasmonic acid; oxIAA, oxidized IAA; SA, salicylic acid.

Arabidopsis *Remorin 1.3* (*REM1.3*) regulating lipid raft microdomain organization in the plasma membrane. These three genes are potentially regulated by the secondary cell wall integrity impairment signals *in situ*.

To further explore transcriptomic changes in the transgenic lines, we carried out a WGCNA (Horvath, 2011) in the cambium/phloem and developing xylem tissues. This analysis groups genes with highly correlated expression patterns into color-coded clusters. The expression of each cluster is then summarized using the eigengene values which serve to create dendrograms showing similarities among the samples and to analyze correlations to external sample traits, in our case growth, SilviScan, hormonomics, and metabolomics data. The WGCNA clusters for three hierarchical levels are shown in Fig. 7A. The co-regulated genes for the middle level of clustering are listed in Supplementary Tables S6 and S7 for the cambium/phloem and

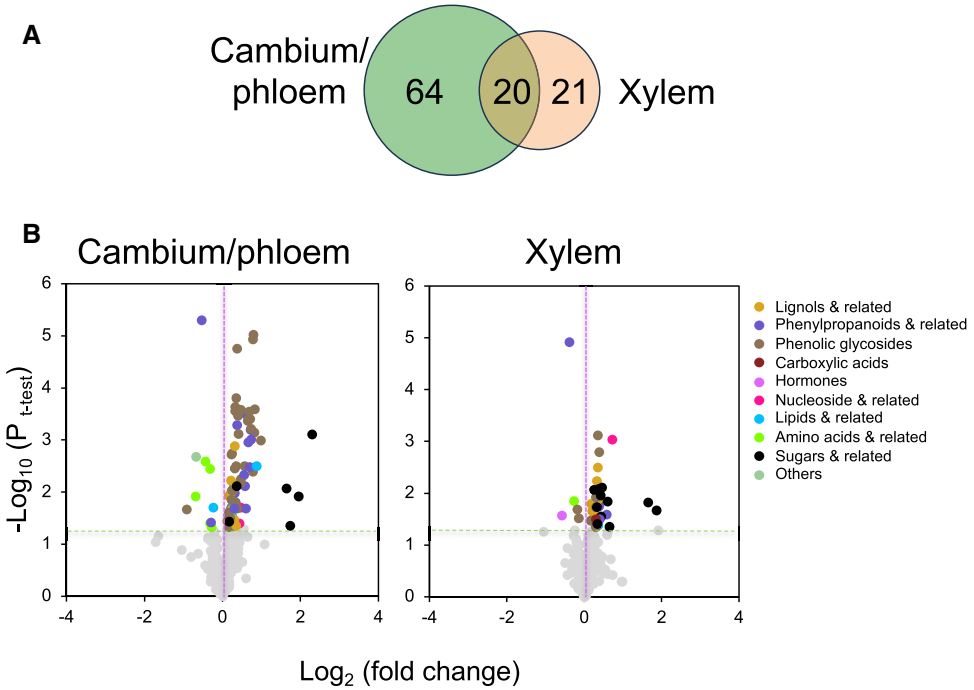

Fig. 5. Metabolomes of cambium/phloem and developing xylem in transgenic lines with altered xylan and increased growth show changes in several groups of compounds. (A) Venn diagram showing the number of metabolites affected in transgenic lines in cambium/phloem and developing xylem tissues out of 300 detected metabolites. (B) Volcano plots of metabolites analyzed by LC-MS and GC-MS showing groups of compounds significantly affected ($P \leq 0.05$, *t*-test) in samples of transgenic lines (WP:GH67, WP:GH10, WP:*Pc*GCE, and WP:GT43-rnai) taken together compared with the wild type. Data are based on eight wild-type trees and four transgenic trees in each line and tissue. The list of affected compounds is given in Supplementary Table S4.

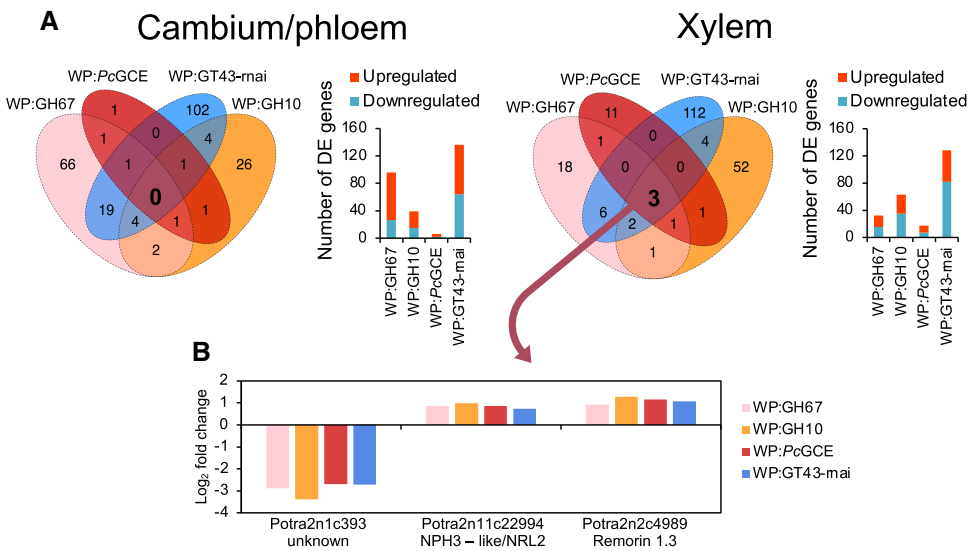

Fig. 6. RNA sequencing of wood-forming tissues in xylan-modified lines with increased growth. (A) Venn diagrams showing numbers of differentially expressed (DE) genes compared with the wild type (WT) in each line ($P_{adj} \leq 0.01$, $|\log_2(\text{fold change}) \geq 0.584$) and bar charts showing the numbers of up- and down-regulated genes in each line. (B) The differential expression of three genes affected in common in the xylem of transgenic lines.

xylem tissues, respectively. In the cambium/phloem, 14 clusters were detected (Fig. 7B), and one of them, the Tan cluster, grouped all transgenic samples separate from the wild-type samples (Fig. 7C; Supplementary Fig. S1). Among the external variables correlated with the eigengene values of the Tan cluster, there were internode length, phenylalanine, many different

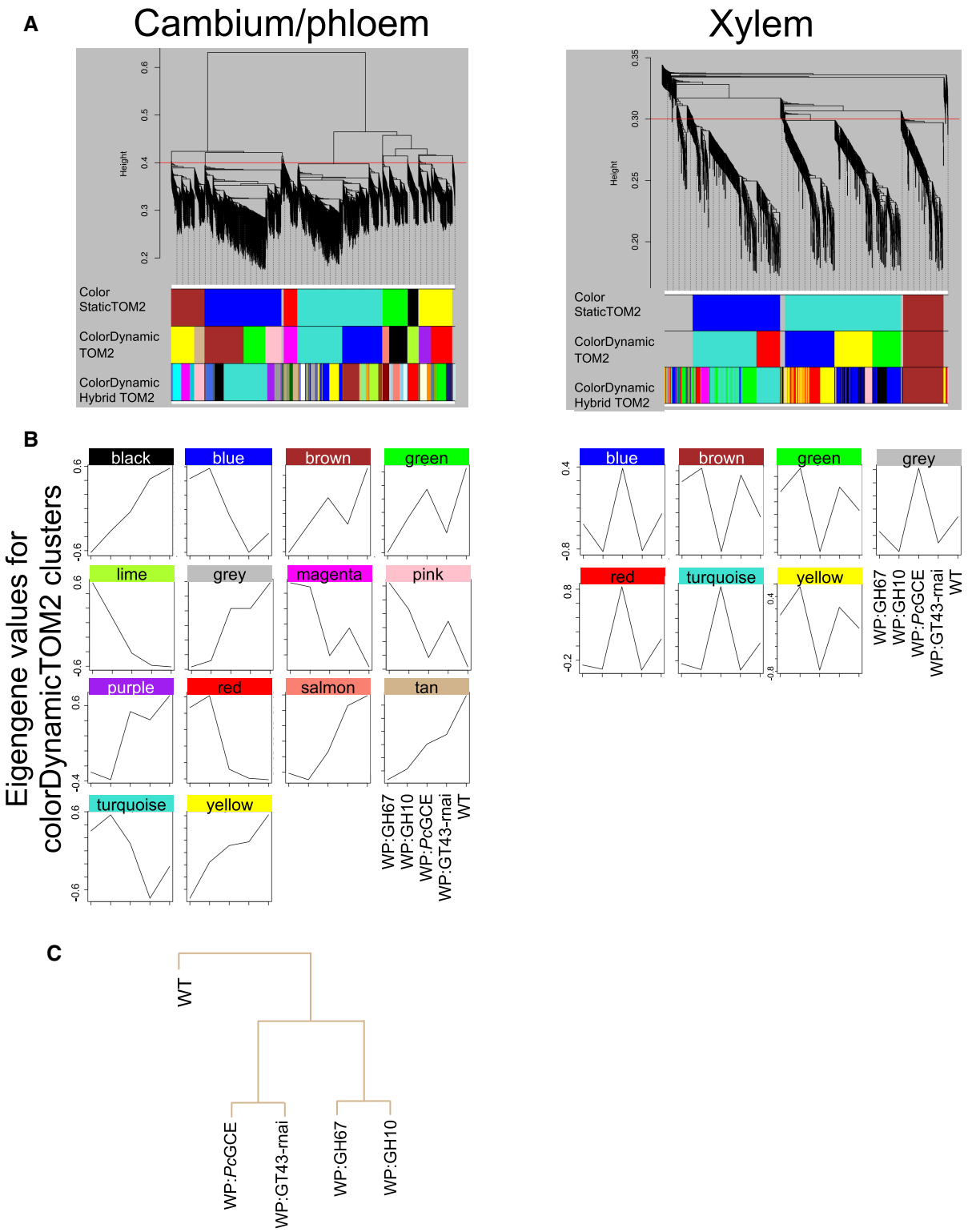

Fig. 7. Clustering of genes based on correlations in different xylan-modified lines and among metabolomics, hormonomics, SilviScan, and growth data. (A) Gene clusters, shown as dendograms for cambium/phloem and developing xylem tissues, obtained by weighted gene correlation network analysis (WGCNA). The color rows below the dendrograms indicate module membership identified by three different methods: the ColorStatic method (first band), the ColorDynamic method (second band), and the ColorDynamicHybrid method (third band). (B) The patterns of gene expression in the different lines for the clusters of the second band. (C) A dendrogram of the Tan cluster showing the grouping of genotypes of transgenic lines, separately from the wild type (WT).

phenylpropanoids, and the hormones *tZ* and IAA (Supplementary Table S8). In the xylem samples, seven gene clusters were detected, but no grouping could be found separating transgenic lines from the wild type (Fig. 7B; Supplementary Fig. S2).

We further analyzed if the genes of the Tan cluster were co-regulated during normal wood formation in aspen using the gene network analysis tool and AspWood dataset (Sundell *et al.*, 2017) available at the PlantGenIE website (https://plantgenie.org/). This detected three gene networks, named Tan 1, Tan 2, and Tan 3, grouping 21, 22, and 88 genes, respectively (Fig. 8; Supplementary Table S9). The Tan 1 network grouped genes that tended to be down-regulated in transgenic lines, but very few of them were significantly down-regulated [$P_{adj} \leq 0.01$, $|\log_2(\text{fold change})| \geq 0.584$]. It was dominated by genes encoding mitochondrial proteins essential for respiration and ROS production. It also included homologs of Arabidopsis genes having function in ABA signaling, *RGLG1* (Wu *et al.*, 2016) and *SCD2* (Hou and Shen, 2020), which was consistent with the decreased levels of ABA in the cambium/phloem tissues (Fig. 4). Moreover, the Tan 1 network contained important developmental regulators, a homolog of *VND1*, a NAC transcription factor triggering differentiation of tracheary elements and secondary wall formation (Ohashi-Ito *et al.*, 2024), *ARF3* regulating meristem size (Sang *et al.*, 2022), and *ANGUSTIFOLIA* (*AN*) regulating polar cell growth (Chen *et al.*, 2022) and homeostasis between SA and JA/ethylene levels (Xie *et al.*, 2020). The Tan 2 network (Fig. 8; Supplementary Table S9) grouped genes that tended to be up-regulated in transgenic lines. It included homologs of regulators of vascular tissue development, *VPNB1* (Podia *et al.*, 2018), *CLAVATA1* (*CLV1*; Zhang *et al.*, 2024), and *ALTERED PHLOEM DEVELOPMENT* (*APL*; Bonke *et al.*, 2003), and genes related to phloem function, such as a homolog of *CALLOSE SYNTHASE 7* (*CalS7*; Xie *et al.*, 2011), and two sucrose synthase-encoding genes, *PtSUS5* and *PtSUS6* (Kumar *et al.*, 2019). It also contained other potential developmental regulators such as *NAC028* and *SQUAMOSA PROMOTER-BINDING PROTEIN LIKE4* (*SPL4*) as well as several genes encoding ankyrin repeat proteins. The Tan 3 network was the largest and it included genes having a weak tendency for down-regulation in transgenic lines. Most of them were encoding ribosomal proteins and proteins related to translation (Fig. 8; Supplementary Table S9). The remaining genes of this network were involved in the regulation of secondary growth, for example regulation of cell division and meristem size, such as cyclin D (*CYCD3;3*; Dewitte *et al.*, 2007), *PROHIBITIN3* (*PHB3*; Kong *et al.*, 2018), and histone deacetylase (*HDA3/HDT1*; Zhang *et al.*, 2019), and signaling, such as homologs of *RACK1B* involved in ABA responses (Guo and Sun, 2017) and *ETO1* limiting ethylene biosynthesis by targeting a subset of ACC synthases to ubiquitination (Lee *et al.*, 2021). Incidentally, three ubiquitin ligase-related genes were in this network, homologs of *PEX10* (Burkhart *et al.*, 2014), *AIRP2* (Cho *et al.*, 2011), and *AT1G30070* (Fig. 8; Supplementary Table S9). The genes identified in these three networks constitute candidates for the fine-tuning of gene expression in the cambial tissues in response to signals from adjacent xylem cells depositing secondary walls.

Discussion

Despite many papers reporting effects of secondary wall integrity impairments on various physiological responses, it is still unclear if there are common physiological responses and common signaling pathways that link the different secondary wall defects to specific outcomes. Here, we addressed this question by investigating the physiological and molecular consequences of different types of xylan alterations in the secondary walls in hybrid aspen.

Xylan is a key hemicellulose of secondary wall layers in angiosperms. Based on extensive analyses of Arabidopsis, it is known that mutants defective in xylan biosynthetic genes affect growth to various degrees depending on redundancy, gene dosage, and the type of xylan defect. Mutants defective in meGlcA side chains have no or a much more attenuated effect on growth compared with mutants in the xylan backbone or acetylation which can be dwarf (Wu *et al.*, 2009, 2010; Lee *et al.*, 2010; Mortimer *et al.*, 2010; Ramírez and Pauly, 2019). Here, we compared effects of fungal hydrolases targeting either the xylan backbone or the meGlcA side chain, either ubiquitously or specifically in cells forming secondary walls in aspen. As in Arabidopsis, the observed effects on growth were variable, with xylanases having a more detrimental effect than an α-glucuronidase, and the severity of growth inhibition depending on xylanase expression levels (Fig. 1). However, unlike in Arabidopsis, we observed that, in some instances, the growth of entire plants was stimulated by xylan impairment, confirming previous observations (Biswal *et al.*, 2015; Derba-Maceluch *et al.*, 2015; Ratke *et al.*, 2018). This occurred only when hydrolases or suppression of native xylan biosynthetic genes were targeted specifically to cells depositing secondary walls, and it concerned 30% of such lines, whereas in 95% of lines with ubiquitously targeted xylan modification the growth was inhibited. This suggests that primary and secondary wall integrity impairments can have opposite effects on growth. Indeed, the primary wall impairments reportedly inhibited growth (Hématy *et al.*, 2007; Gigli-Bisceglia *et al.*, 2018; Dünser *et al.*, 2019; Sampathkumar *et al.*, 2019). Inhibition of cell division is thought to be mediated by a pathway dependent on nitrate and cytokinin reductases controlling cytokinin levels (Gigli-Bisceglia *et al.*, 2018), whereas inhibition of cell expansion is controlled by *THE1*- or *FER*-mediated pathways (Hématy *et al.*, 2007; Dünser *et al.*, 2019). To identify molecular players involved in growth stimulation induced by secondary wall impairment, we used hormonomics, metabolomics, and transcriptomics analyses in the xylem cells depositing secondary walls (i.e. at the site of

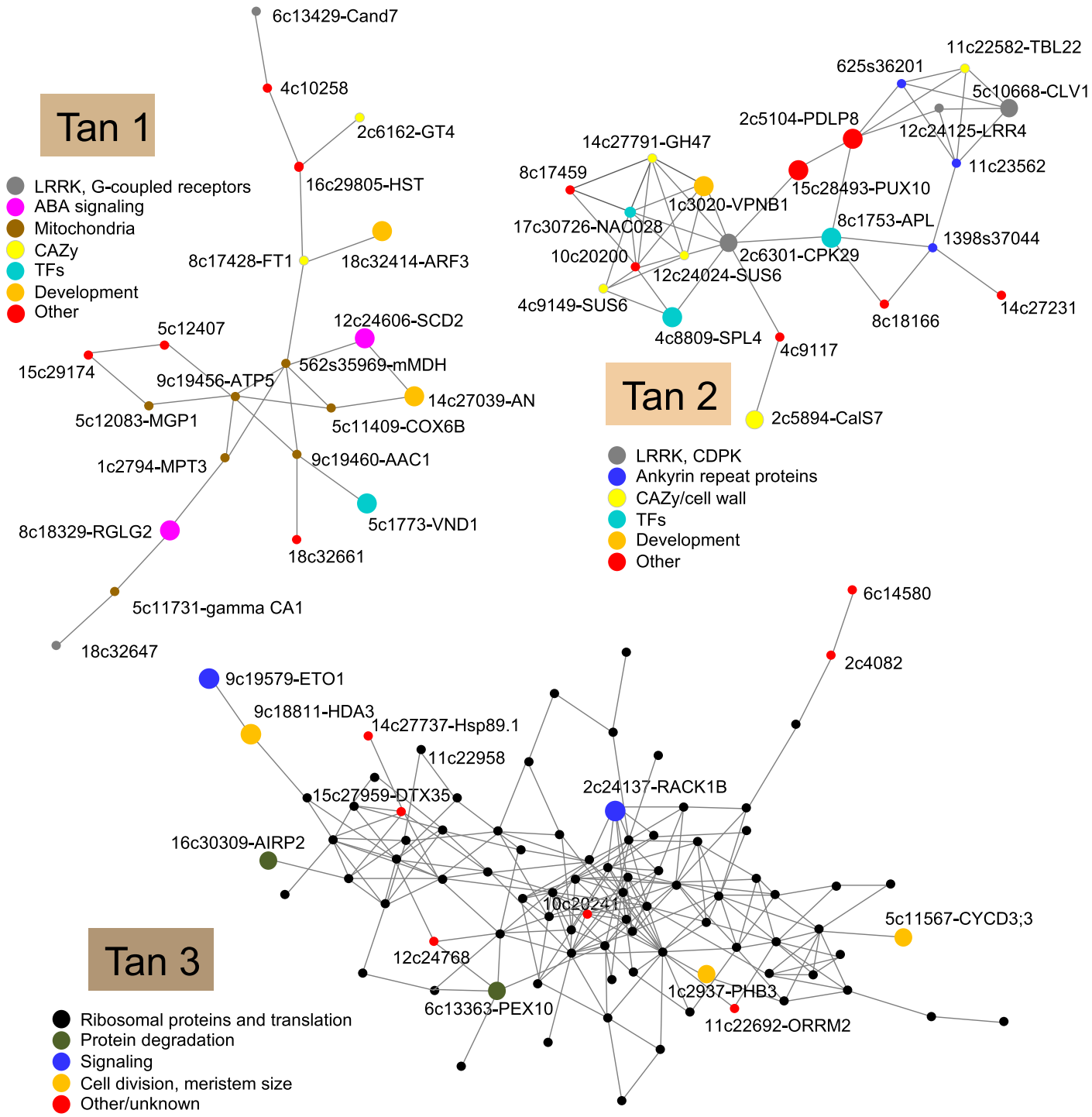

Fig. 8. Co-expression networks of genes of WGCNA Tan clusters that were correlated with growth and were distinctively expressed in xylan-modified lines with increased growth compared with the wild type across wood-forming aspen tissues. Data from AspWood (https://plantgenie.org/). Nodes are labeled with the *P. tremula* gene ID that follows 'Potra2n' and Arabidopsis gene name, if identified. In the Tan3 network, the gene codes for ribosomal protein-encoding genes were omitted for clarity. The lists of genes for all networks are given in Supplementary Table S9. Larger node symbols were used for genes discussed in the text.

wall damage perception) and in adjacent cambial region tissues (i.e. where the growth is stimulated). The summary of our findings is presented in Fig. 9.

Expression of three genes was affected at the cell wall damage site (i.e. in the secondary wall-forming xylem) in all xylan-altered lines (Figs 6, 9). Of these, two genes, *REM1.3*

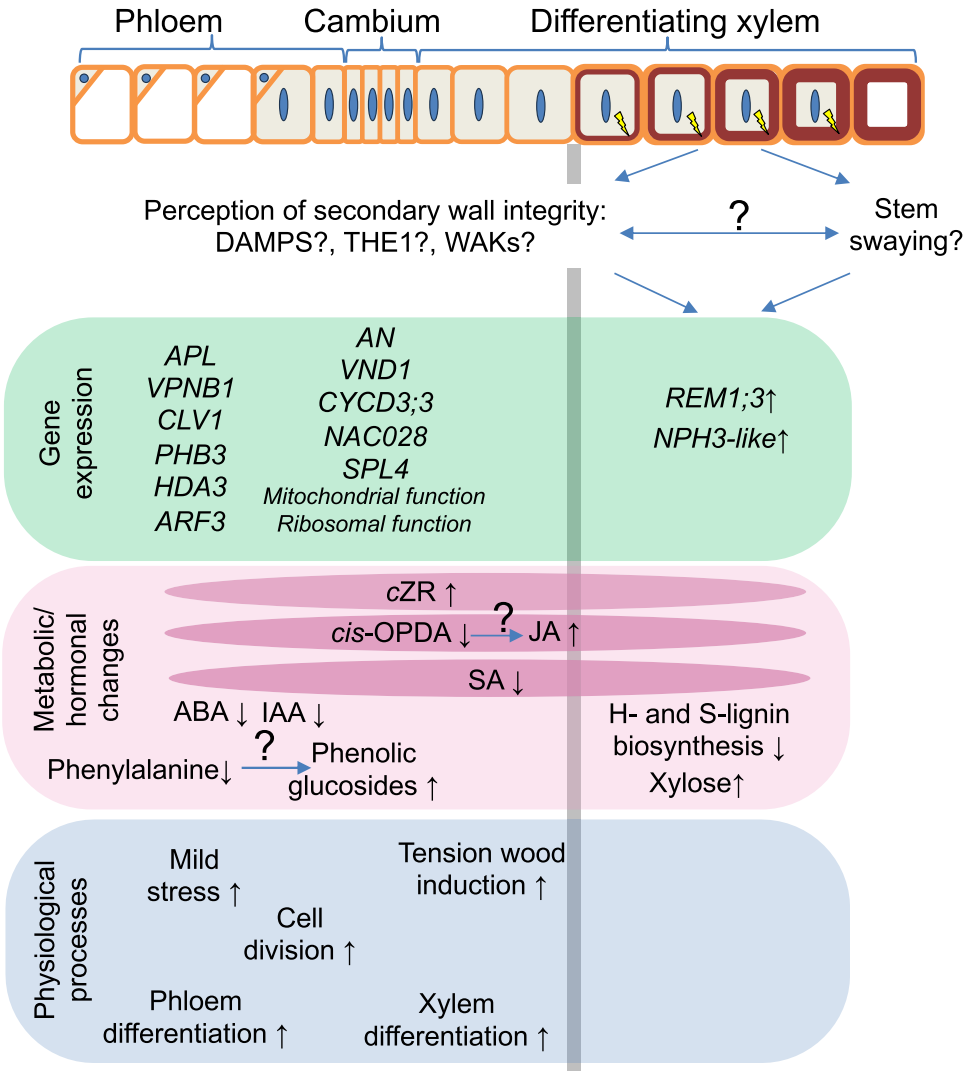

Fig. 9. Diagram illustrating changes in the physiological processes, metabolic/hormonal status, and gene expression which are induced in wood-forming tissues when secondary cell wall xylan is mildly modified. Increased stem swaying is expected when xylan integrity is impaired, but the relationship between the stem swaying reaction and putative secondary cell wall defect perception is unknown. We suggest that DAMPs such as oligogalacturonides and/or xylobiose (Dewangan *et al.*, 2023; Sivan *et al.*, 2025) are involved in the integrity perception, along with receptors such as THE1 and WAKs. The subsequent signaling induces *REM1;3* and *NPH3*-like genes in the xylem that could further regulate the cell wall integrity responses. Hormonal changes that can occur in both cambium/phloem and developing xylem tissues (marked by darker pink ovals) include a conversion of *cis*-OPDA to JA, a decrease in SA, possibly resulting from decreased biosynthesis in the phloem, and an increase in *c*ZR that is probably transported from the phloem. ABA and IAA decrease in the cambium/phloem. Tension wood is induced in differentiating xylem. Farther in the cambial region tissues, cell division and xylem/phloem differentiation are activated. Phenylalanine might be converted into phenolic glycosides, indicating a possible stress response. Genes responding in the cambium/phloem are related to mitochondrial and ribosomal functions, cell cycle, meristem size regulation, and vascular differentiation. The gray vertical line indicates the approximate split between cambium/phloem and differentiating xylem tissues that were analyzed.

encoding remorin and *NRL2* of the *NPH3* family, were up-regulated in transgenic lines and they are of particular interest. Remorins are essential for lipid raft organization and symplasmic signaling. In Arabidopsis, REM1.3 protein is rapidly phosphorylated by the CALCIUM-DEPENDENT PROTEIN KINASE 3 (CDPK3) (Perraki *et al.*, 2018) in response to oligogalacturonides (Kohorn *et al.*, 2016), which regulates nanodomain organization and restricts plasmodesmatal transport downstream of SA signaling (Huang *et al.*, 2019). The decreased SA concentration observed in transgenic lines (Figs 4, 9) would then increase symplasmic transport. Regulation of symplasmic transport is relevant in the case of secondary wall integrity signaling because cell wall damage perception must occur specifically during deposition of the secondary wall layer, namely when cell growth is already finished, and its perception needs to induce a mobile signal transmitted to the dividing and growing cells, and possibly spreading to other organs to affect growth. Another gene up-regulated in all

studied xylan-modified lines was a homolog of *NRL2* from the *NPH3* family which encodes proteins interacting with blue-light receptor-like kinases called phototropins and mediating blue-light phototropic responses (Christie *et al.*, 2018). NRL2 protein was found to interact with PHOTOTROPIN 1 (PHO1) but the interaction was not affected by light (Sullivan *et al.*, 2009), suggesting a role in a process other than light signaling. Therefore, both *REM1.3* and *NRL2* are key candidates for secondary wall integrity sensing and signaling, which leads to better growth, and should be further analyzed.

Many changes in metabolites and hormones were observed in common between the cambium/phloem and xylem samples (Figs 4, 9). This could be related to increased symplasmic transport, as discussed above, or to increased apoplasmic transport due to a cell wall defect. Among the most notable changes in hormonal status in lines with impaired xylan there was a tendency for an increase in JA and a decrease in its precursor, *cis*-OPDA, which could indicate increased biosynthesis of active jasmonates in the developing xylem (Fig. 4). This increase could play a role in growth stimulation observed in the transgenic lines as JA is known for its stimulatory effect on cambial divisions and xylem formation (Sehr *et al.*, 2010; Jang *et al.*, 2017). Decreased ABA levels in the transgenic lines (Fig. 4) could also play an important role in secondary wall integrity signaling. ABA is known for its growth inhibitory effects (Popko *et al.*, 2010). Strongly decreased ABA levels accompanied enhanced cambial activity and phloem production in lines with severe secondary cell wall damage (Sivan *et al.*, 2025). Recently, cell wall damage induced by isoxaben was observed in the central part of the Arabidopsis root, corresponding to the stele, where it was shown to induce THE1 that mediated JA signaling (Bacete *et al.*, 2022). The treatment also reduced ABA in adjacent tissues, again in a THE1-dependent manner. These observations, along with the data presented herein, strongly implicate reduced ABA and increased JA signaling downstream of THE1 as a common response to secondary cell wall defects.

Interestingly, similar changes in the hormones (decreased *cis*-OPDA and reduced ABA concentrations) were observed in wood-forming tissues of stems subjected to stem swaying (Urbancsok *et al.*, 2023). This treatment also stimulated plant growth and xylem production. Moreover, it induced increased formation of tension wood, similar to effects of xylan impairment (Figs 2, 9). These similarities indicate that pathways between mechanical stress perception during stem swaying and secondary cell wall damage overlap and possibly the changes reported here in the xylan-modified plants are mediated via stem swaying. It would therefore be crucial to determine if the stem swaying is needed for growth stimulation in secondary wall integrity-compromised plants. Secondary wall damage perception probably also involves DAMPs such as xylobiose (Dewangan *et al.*, 2023), as found in the case of xylanase-overexpressing aspen (Sivan *et al.*, 2025). Here we found that aspen with xylan defects and increased growth showed increases in xylose and derived sugars (Supplementary Table S4) which could originate from xylobiose or xylan. Oligogalacturonides could also play a role as DAMPs when xylan integrity is altered, because xylan and pectin networks are likely to be interconnected in the wood (Biswal *et al.*, 2014).

At the site of increased growth (i.e. in the cambial region tissues), transcriptomic changes were subtle, but the WGCNA clustering identified the Tan cluster of co-regulated transcripts in transgenic lines which correlated with growth-promoting hormones, such as IAA and *t*Z, and metabolites related to amino acids and phenylpropanoids (Fig. 7; Supplementary Tables S6, S8). These results support common genetic machinery responsible for growth stimulation. Interestingly, these genes formed co-expression networks during the normal process of xylogenesis (Fig. 8; Supplementary Table S9), which could operate during the monitoring of secondary wall integrity and fine-tuning of xylogenesis with growth. This fine-tuning appears to specifically regulate different groups of genes. One of them represents phloem biogenesis-related genes illustrated by the Tan 2 network, grouping genes related to vascular development, phloem fate specification, and phloem function. Incidentally, our previous analyses showed increased phloem production when xylan structure was heavily affected (Sivan *et al.*, 2025). Another group represents genes regulating mitochondrial function as exemplified by the Tan 1 network (Fig. 8; Supplementary Table S9). This is particularly intriguing given that the defects in mitochondrial functions were shown to confer the resistance to cell wall damage caused by inhibition of cellulose biosynthesis (Hu *et al.*, 2016).

Among the most commonly increased metabolites in transgenic lines were phenyl glycosides (Figs 5, 9; Supplementary Table S4) which are known to accompany biotic stress responses (Babst *et al.*, 2010). Thus, the modification of xylan could result in activation of biotic stress responses, as also known for other cases of secondary wall impairment (Hernández-Blanco *et al.*, 2007; Gallego-Giraldo *et al.*, 2011a; Pogorelko *et al.*, 2013; Pawar *et al.*, 2016; Molina *et al.*, 2021).

In conclusion, we demonstrated that common physiological, hormonal, metabolic, and transcriptional responses are activated in wood-forming tissues when xylan is impaired in developing secondary walls (Fig. 9). How cell wall defects are perceived in the xylem cells is still unknown, but we have identified two genes, *REM1;3* and *NRL2*, which are induced in the xylem upon secondary wall xylan damage and could regulate downstream responses to impaired secondary walls. These responses are partially non-cell-autonomous, involving changes in the cambial meristem and further affecting growth of entire plants. The identified genes and hormones probably coordinate the process of secondary wall formation with cambial activity and vascular differentiation during secondary growth.

Supplementary data

The following supplementary data are available at *JXB* online.

Fig. S1. Analysis of transcriptomic changes in the cambium/phloem tissues of transgenic lines compared with the wild type using WGNCA.

Fig. S2. Analysis of transcriptomic changes in the xylem tissue of transgenic lines compared with the wild type using WGNCA.

Protocol S1. Details of metabolomics analyses.

Table S1. Primers used in this study.

Table S2. Levels of all compounds detected by hormonomics analysis in developing wood tissues of the selected transgenic lines with modified xylan and increased growth.

Table S3. SilviScan wood traits that were not affected in the selected transgenic lines with modified xylan and increased growth.

Table S4. All compounds detected by metabolomics analysis in developing wood tissues of the transgenic lines with modified xylan and increased growth.

Table S5. Genes differentially expressed ($|\log_2$ (fold change)$| \geq 0.584$ and $P_{adj} \leq 0.01$) in wood-forming tissues of at least one transgenic line compared with the wild type.

Table S6. Clusters of genes co-regulated in the cambium/developing phloem of transgenic lines and the wild type according to WGCNA.

Table S7. Clusters of gene co-regulated in the xylem of transgenic lines and wild type according to WGCNA.

Table S8. WGCNA clusters of co-regulated genes correlated with different variables corresponding to growth, hormones, and metabolites.

Table S9. Co-expression networks in the wood-forming aspen tissues for the Tan WGCNA cluster of co-regulated genes correlated with different variables including growth, hormones, and metabolites.

Acknowledgements

We acknowledge the Umeå Plant Science Centre (UPSC) Tree Phenotyping Platform, Bioinformatics Facility, Microscopy Facility, Biopolymer Analytical Platform, and the Swedish Metabolomics Centre in Umeå (www.swedishmetabolomicscentre.se). We thank Thomas Grahn (RISE) for help with NIR estimations of tension wood.

Author contributions

JU: supervised the experiments, processed wood material, extracted RNA, analyzed transgene expression, and prepared samples for omics analyses; END: analyzed roots, designed and performed bioinformatic analyses, and prepared figures; MDM: created transgenic aspen and collected samples for SilviScan analysis; PS: performed wood chemistry analyses; JU, END, and FRB: carried out the greenhouse experiment and tree phenotyping; MM: analyzed metabolomics data and prepared them for publication; ZY and GS: carried out wood SilviScan and NIR analyses; JŠ, KC, and MK: analyzed hormones and related compounds; EJM: designed and coordinated the research, secured the funding, and wrote the paper with contributions from all authors.

Conflict of interest

The authors declare no conflict of interest.

Funding

This work was supported by the Knut and Alice Wallenberg (KAW) Foundation, the Swedish Governmental Agency for Innovation Systems (VINNOVA), Swedish Research Council, Kempestiftelserna, T4F, Bio4Energy, and the SSF program ValueTree RBP14-0011 to EJM. MK was supported by The Czech Science Foundation (GAČR) via junior grant 20-25948Y. END was partially supported by project SCWpriming (grant no. КП-06-ДБ/2 from 14.12.2023) of the Bulgarian national research program 'Petar Beron i NIE', and BG16RFPR002-1.014-0003-C01, financed by the European Regional Development Fund through the Bulgarian Program for Research, Innovation, and Digitalisation for Smart Transformation (PRIDST).

Data availability

The raw RNA-seq data that support the findings of this study are available in the European Nucleotide Archive (ENA) at EMBL-EBI (https://www.ebi.ac.uk/ena/browser/home), under accession ID PRJEB82792.

References

Babst BA, Harding SA, Tsai CJ. 2010. Biosynthesis of phenolic glycosides from phenylpropanoid and benzenoid precursors in *Populus*. Journal of Chemical Ecology **36**, 286–297.

Bacete L, Schulz J, Engelsdorf T, ***et al.*** 2022. THESEUS1 modulates cell wall stiffness and abscisic acid production in *Arabidopsis thaliana*. Proceedings of the National Academy of Sciences, USA **119**, e2119258119.

Barbut FR, Cavel E, Donev EN, ***et al.*** 2024. Integrity of xylan backbone affects plant responses to drought. Frontiers in Plant Science **15**, 1422701.

Biswal AK, Hao Z, Pattathil S, ***et al.*** 2015. Downregulation of GAUT12 in *Populus deltoides* by RNA silencing results in reduced recalcitrance, increased growth and reduced xylan and pectin in a woody biofuel feedstock. Biotechnology for Biofuels **8**, 41.

Biswal AK, Soeno K, Latha Gandla M, ***et al.*** 2014. Aspen pectate lyase PtxtPL1-27 mobilizes matrix polysaccharides from woody tissues and improves saccharification yield. Biotechnology for Biofuels **7**, 11.

Bonawitz ND, Kim JI, Tobimatsu Y, ***et al.*** 2014. Disruption of Mediator rescues the stunted growth of a lignin-deficient *Arabidopsis* mutant. Nature **509**, 376–380.

Bonke M, Thitamadee S, Mähönen AP, Hauser MT, Helariutta Y. 2003. APL regulates vascular tissue identity in *Arabidopsis*. Nature **426**, 181–186.

Bosca S, Barton CJ, Taylor NG, Ryden P, Neumetzler L, Pauly M, Roberts K, Seifert GJ. 2006. Interactions between *MUR10/CesA7*-dependent secondary cellulose biosynthesis and primary cell wall structure. Plant Physiology **142**, 1353–1363.

Burkhart SE, Kao YT, Bartel B. 2014. Peroxisomal ubiquitin-protein ligases peroxin2 and peroxin10 have distinct but synergistic roles in matrix protein import and peroxin5 retrotranslocation in *Arabidopsis*. Plant Physiology **166**, 1329–1344.

Chang S, Puryear J, Cairney J. 1993. A simple and efficient method for isolating RNA from pine trees. Plant Molecular Biology Reporter **11**, 113–116.

Chen B, Dang X, Bai W, ***et al.*** 2022. The IPGA1–ANGUSTIFOLIA module regulates microtubule organisation and pavement cell shape in *Arabidopsis*. New Phytologist **236**, 1310–1325.

Chen Z, Hong X, Zhang H, Wang Y, Li X, Zhu JK, Gong Z. 2005. Disruption of the cellulose synthase gene, *AtCesA8/IRX1*, enhances drought and osmotic stress tolerance in *Arabidopsis*. Plant Journal **43**, 273–283.

Cho SK, Ryu MY, Seo DH, Kang BG, Kim WT. 2011. The Arabidopsis RING E3 ubiquitin ligase AtAIRP2 plays combinatory roles with AtAIRP1 in abscisic acid-mediated drought stress responses. Plant Physiology **157**, 2240–2257.

Chong SL, Koutaniemi S, Virkki L, Pynnönen H, Tuomainen P, Tenkanen M. 2013. Quantitation of 4-*O*-methylglucuronic acid from plant cell walls. Carbohydrate Polymers **91**, 626–630.

Christie JM, Suetsugu N, Sullivan S, Wada M. 2018. Shining light on the function of NPH3/RPT2-like proteins in phototropin signaling. Plant Physiology **176**, 1015–1024.

Derba-Maceluch M, Awano T, Takahashi J, ***et al.*** 2015. Suppression of xylan endotransglycosylase *PtxtXyn10A* affects cellulose microfibril angle in secondary wall in aspen wood. New Phytologist **205**, 666–681.

Derba-Maceluch M, Mitra M, Hedenström M, ***et al.*** 2023. Xylan glucuronic acid side chains fix suberin-like aliphatic compounds to wood cell walls. New Phytologist **238**, 297–312.

Dewangan BP, Gupta A, Sah RK, Das S, Kumar S, Bhattacharjee S, Pawar PA. 2023. Xylobiose treatment triggers a defense-related response and alters cell wall composition. Plant Molecular Biology **113**, 383–400.

Dewitte W, Scofield S, Alcasabas AA, ***et al.*** 2007. *Arabidopsis* CYCD3 D-type cyclins link cell proliferation and endocycles and are rate-limiting for cytokinin responses. Proceedings of the National Academy of Sciences, USA **104**, 14537–14542.

Doblas VG, Gonneau M, Höfte H. 2018. Cell wall integrity signaling in plants: malectin-domain kinases and lessons from other kingdoms. Cell Surface **3**, 1–11.

Donev EN, Derba-Maceluch M, Liu X-K, ***et al.*** 2025. Glucuronoyl esterase of pathogenic *Phanerochaete carnosa* induces immune responses in aspen independently of its enzymatic activity. Plant Biotechnology Journal [in press]. https://doi.org/10.1111/pbi.70357.

Dünser K, Gupta S, Herger A, Feraru MI, Ringli C, Kleine-Vehn J. 2019. Extracellular matrix sensing by FERONIA and leucine-rich repeat extensins controls vacuolar expansion during cellular elongation in *Arabidopsis thaliana*. The EMBO Journal **38**, e100353.

Engelsdorf T, Gigli-Bisceglia N, Veerabagu M, McKenna JF, Vaahtera L, Augstein F, Van der Does D, Zipfel C, Hamann T. 2018. The plant cell wall integrity maintenance and immune signaling systems cooperate to control stress responses in *Arabidopsis thaliana*. Science Signaling **11**, eaao3070.

Gallego-Giraldo L, Escamilla-Trevino L, Jackson LA, Dixon RA. 2011b. Salicylic acid mediates the reduced growth of lignin down-regulated plants. Proceedings of the National Academy of Sciences, USA **108**, 20814–20819.

Gallego-Giraldo L, Jikumaru Y, Kamiya Y, Tang Y, Dixon RA. 2011a. Selective lignin downregulation leads to constitutive defense response expression in alfalfa (*Medicago sativa* L.). New Phytologist **190**, 627–639.

Gallego-Giraldo L, Liu C, Pose-Albacete S, ***et al.*** 2020. ARABIDOPSIS DEHISCENCE ZONE POLYGALACTURONASE 1 (ADPG1) releases latent defense signals in stems with reduced lignin content. Proceedings of the National Academy of Sciences, USA **117**, 3281–3290.

Gerber L, Eliasson M, Trygg J, Moritz T, Sundberg B. 2012. Multivariate curve resolution provides a high-throughput data processing pipeline for pyrolysis–gas chromatography/mass spectrometry. Journal of Analytical and Applied Pyrolysis **95**, 95–100.

Gigli-Bisceglia N, Engelsdorf T, Strnad M, ***et al.*** 2018. Cell wall integrity modulates *Arabidopsis thaliana* cell cycle gene expression in a cytokinin- and nitrate reductase-dependent manner. Development **145**, dev166678.

Gullberg J, Jonsson P, Nordström A, Sjöström M, Moritz T. 2004. Design of experiments: an efficient strategy to identify factors influencing extraction and derivatization of *Arabidopsis thaliana* samples in metabolomic studies with gas chromatography/mass spectrometry. Analytical Biochemistry **331**, 283–295.

Guo R, Sun W. 2017. Sumoylation stabilizes RACK1B and enhance its interaction with RAP2.6 in the abscisic acid response. Scientific Reports **7**, 44090.

Hématy K, Sado PE, Van Tuinen A, Rochange S, Desnos T, Balzergue S, Pelletier S, Renou JP, Höfte H. 2007. A receptor-like kinase mediates the response of Arabidopsis cells to the inhibition of cellulose synthesis. Current Biology **17**, 922–391.

Hernández-Blanco C, Feng DX, Hu J, ***et al.*** 2007. Impairment of cellulose synthases required for *Arabidopsis* secondary cell wall formation enhances disease resistance. The Plant Cell **19**, 890–903.

Horvath S. 2011. Weighted network analysis applications in genomics and systems biology. New York: Springer-Verlag.

Hou B, Shen Y. 2020. A clathrin-related protein, SCD2/RRP1, participates in abscisic acid signaling in Arabidopsis. Frontiers in Plant Science **11**, 892.

Hu Z, Vanderhaeghen R, Cools T, ***et al.*** 2016. Mitochondrial defects confer tolerance against cellulose deficiency. The Plant Cell **28**, 2276–2290.

Huang D, Sun Y, Ma Z, ***et al.*** 2019. Salicylic acid-mediated plasmodesmal closure via Remorin-dependent lipid organization. Proceedings of the National Academy of Sciences, USA **116**, 21274–21284.

Jang G, Chang SH, Um TY, Lee S, Kim JK, Choi YD. 2017. Antagonistic interaction between jasmonic acid and cytokinin in xylem development. Scientific Reports **7**, 10212.

Kákošová A, Digonnet C, Goffner D, Lišková D. 2013. Galactoglucomannan oligosaccharides are assumed to affect tracheary element formation via interaction with auxin in *Zinnia* xylogenic cell culture. Plant Cell Reports **32**, 479–487.

Karady M, Hladík P, Cermanová K, Jiroutová P, Antoniadi I, Casanova-Sáez R, Ljung K, Novák O. 2024. Profiling of 1-aminocyclopropane-1-carboxylic acid and selected phytohormones in *Arabidopsis* using liquid chromatography–tandem mass spectrometry. Plant Methods **20**, 41.

Kohorn BD. 2016. Cell wall-associated kinases and pectin perception. Journal of Experimental Botany **67**, 489–494.

Kohorn BD, Hoon D, Minkoff BB, Sussman MR, Kohorn SL. 2016. Rapid oligo-galacturonide induced changes in protein phosphorylation in Arabidopsis. Molecular & Cellular Proteomics **15**, 1351–1359.

Kong X, Tian H, Yu Q, ***et al.*** 2018. PHB3 maintains root stem cell niche identity through ROS-responsive AP2/ERF transcription factors in Arabidopsis. Cell Reports **22**, 1350–1363.

Kumar V, Hainaut M, Delhomme N, Mannapperuma C, Immerzeel P, Street NR, Henrissat B, Mellerowicz EJ. 2019. Poplar carbohydrate-active enzymes: whole-genome annotation and functional analyses based on RNA expression data. The Plant Journal **99**, 589–609.

Langfelder P, Horvath S. 2008. WGCNA: an R package for weighted correlation network analysis. BMC Bioinformatics **9**, 559.

Latha Gandla M, Derba-Maceluch M, Liu X, Gerber L, Master ER, Mellerowicz EJ, Jönsson LJ. 2015. Expression of a fungal glucuronoyl esterase in Populus: effects on wood properties and saccharification efficiency. Phytochemistry **112**, 210–220.

Lee HY, Park HL, Park C, Chen YC, Yoon GM. 2021. Reciprocal antagonistic regulation of E3 ligases controls ACC synthase stability and responses to stress. Proceedings of the National Academy of Sciences, USA **118**, e2011900118.

Lee C, Teng Q, Huang W, Zhong R, Ye ZH. 2010. The Arabidopsis family GT43 glycosyltransferases form two functionally nonredundant groups essential for the elongation of glucuronoxylan backbone. Plant Physiology **153**, 526–541.

Liu C, Yu H, Voxeur A, Rao X, Dixon RA. 2023. FERONIA and wall-associated kinases coordinate defense induced by lignin modification in plant cell walls. Science Advances **9**, eadf7714.

Mélida H, Bacete L, Ruprecht C, Rebaque D, del Hierro I, López G, Brunner F, Pfrengle F, Molina A. 2020. Arabinoxylan-oligosaccharides act as damage associated molecular patterns in plants regulating disease resistance. Frontiers in Plant Science **11**, 1210.

Molina A, Miedes E, Bacete L, ***et al.*** 2021. Arabidopsis cell wall composition determines disease resistance specificity and fitness. Proceedings of the National Academy of Sciences, USA **118**, e2010243118.

Mortimer JC, Miles GP, Brown DM, ***et al.*** 2010. Absence of branches from xylan in Arabidopsis *gux* mutants reveals potential for simplification of lignocellulosic biomass. Proceedings of the National Academy of Sciences, USA **107**, 17409–17414.

Moussu S, Lee HK, Haas KT, ***et al.*** 2023. Plant cell wall patterning and expansion mediated by protein–peptide–polysaccharide interaction. Science **382**, 719–725.

Ohashi-Ito K, Iwamoto K, Fukuda H. 2024. LONESOME HIGHWAY–TARGET OF MONOPTEROS5 transcription factor complex promotes a pre-differentiation state for xylem vessel differentiation in the root apical meristem

by inducing the expression of *VASCULAR-RELATED NAC-DOMAIN* genes. New Phytologist **242**, 1146–1155.

Pawar PM, Derba-Maceluch M, Chong SL, ***et al.*** 2016. Expression of fungal acetyl xylan esterase in *Arabidopsis thaliana* improves saccharification of stem lignocellulose. Plant Biotechnology Journal **14**, 387–397.

Perraki A, Gronnier J, Gouguet P, ***et al.*** 2018. REM1.3's phospho-status defines its plasma membrane nanodomain organization and activity in restricting PVX cell-to-cell movement. PLoS Pathogens **14**, e1007378.

Pfaffl MW. 2001. A new mathematical model for relative quantification in real-time RT–PCR. Nucleic Acids Research **29**, e45.

Podia V, Milioni D, Katsareli E, Valassakis C, Roussis A, Haralampidis K. 2018. Molecular and functional characterization of *Arabidopsis thaliana VPNB1* gene involved in plant vascular development. Plant Science **277**, 11–19.

Pogorelko G, Lionetti V, Fursova O, Sundaram RM, Qi M, Whitham SA, Bogdanove AJ, Bellincampi D, Zabotina OA. 2013. Arabidopsis and *Brachypodium distachyon* transgenic plants expressing *Aspergillus nidulans* acetylesterases have decreased degree of polysaccharide acetylation and increased resistance to pathogens. Plant Physiology **162**, 9–23.

Popko J, Hänsch R, Mendel RR, Polle A, Teichmann T. 2010. The role of abscisic acid and auxin in the response of poplar to abiotic stress. Plant Biology **12**, 42–58.

Pramod S, Gandla ML, Derba-Maceluch M, Jönsson LJ, Mellerowicz EJ, Winestrand S. 2021. Saccharification potential of transgenic greenhouse- and field-grown aspen engineered for reduced xylan acetylation. Frontiers in Plant Science **12**, 704960.

Ramírez V, Pauly M. 2019. Genetic dissection of cell wall defects and the strigolactone pathway in Arabidopsis. Plant Direct **3**, e00149.

Ramírez V, Xiong G, Mashiguchi K, Yamaguchi S, Pauly M. 2018. Growth- and stress-related defects associated with wall hypoacetylation are strigolactone-dependent. Plant Direct **2**, e00062.

Ratke C, Pawar PM, Balasubramanian VK, Naumann M, Duncranz ML, Derba-Maceluch M, Gorzsás A, Endo S, Ezcurra I, Mellerowicz EJ. 2015. *Populus GT43* family members group into distinct sets required for primary and secondary wall xylan biosynthesis and include useful promoters for wood modification. Plant Biotechnology Journal **13**, 26–37.

Ratke C, Terebieniec BK, Winestrand S, ***et al.*** 2018. Downregulating aspen xylan biosynthetic GT43 genes in developing wood stimulates growth via reprograming of the transcriptome. New Phytologist **219**, 230–245.

Renström A, Scheepers G, Yassin Z, Sivan P, Niittylä T, Mellerowicz EJ, Tuominen H. 2025. High-resolution imaging of the physical and chemical properties of *Populus* stem transversal sections using SilviScan and near-infrared spectroscopy. IAWA Journal **2025**, 1–16.

Sampathkumar A, Peaucelle A, Fujita M, Schuster C, Persson S, Wasteneys GO, Meyerowitz EM. 2019. Primary wall cellulose synthase regulates shoot apical meristem mechanics and growth. Development **146**, dev179036.

Sang Q, Vayssières A, Ó'Maoiléidigh DS, Yang X, Vincent C, Bertran Garcia de Olalla E, Cerise M, Franzen R, Coupland G. 2022. MicroRNA172 controls inflorescence meristem size through regulation of APETALA2 in Arabidopsis. New Phytologist **235**, 356–371.

Schauer N, Steinhauser D, Strelkov S, ***et al.*** 2005. GC-MS libraries for the rapid identification of metabolites in complex biological samples. FEBS Letters **579**, 1332–1337.

Schoenaers S, Lee HK, Gonneau M, ***et al.*** 2024. Rapid alkalinization factor 22 has a structural and signaling role in root hair cell wall assembly. Nature Plants **10**, 494–511.

Sehr EM, Agusti J, Lehner R, Farmer EE, Schwarz M, Greb T. 2010. Analysis of secondary growth in the Arabidopsis shoot reveals a positive role of jasmonate signaling in cambium formation. The Plant Journal **63**, 811–822.

Shannon P, Markiel A, Ozier O, Baliga NS, Wang JT, Ramage D, Amin N, Schwikowski B, Ideker T. 2003. Cytoscape: a software environment for integrated models of biomolecular interaction networks. Genome Research **13**, 2498–2504.

Šimura J, Antoniadi I, Široká J, Tarkowská D, Strnad M, Ljung K, Novák O. 2018. Plant hormonomics: multiple phytohormone profiling by targeted metabolomics. Plant Physiology **177**, 476–489.

Sivan P, Urbancsok J, Donev EN, ***et al.*** 2025. Modification of xylan in secondary walls alters cell wall biosynthesis and wood formation programs and improves saccharification. Plant Biotechnology Journal **23**, 174–197.

Sullivan S, Thomson CE, Kaiserli E, Christie JM. 2009. Interaction specificity of *Arabidopsis* 14-3-3 proteins with phototropin receptor kinases. FEBS Letters **583**, 2187–2193.

Sundell D, Mannapperuma C, Netotea S, Delhomme N, Lin YC, Sjödin A, Van de Peer Y, Jansson S, Hvidsten TR, Street NR. 2015. The plant genome integrative explorer resource: PlantGenIE.org. New Phytologist **208**, 1149–1156.

Sundell D, Street NR, Kumar M, ***et al.*** 2017. AspWood: high-spatial-resolution transcriptome profiles reveal uncharacterized modularity of wood formation in *Populus tremula*. The Plant Cell **29**, 1585–1604.

Urbancsok J, Donev EN, Sivan P, ***et al.*** 2023. Flexure wood formation via growth reprogramming in hybrid aspen involves jasmonates and polyamines and transcriptional changes resembling tension wood development. New Phytologist **240**, 2312–2334.

Vaahtera L, Schulz J, Hamann T. 2019. Cell wall integrity maintenance during plant development and interaction with the environment. Nature Plants **5**, 924–932.

Wang W, Talide L, Viljamaa S, Niittylä T. 2022. Aspen growth is not limited by starch reserves. Current Biology **32**, 3619–3627.

Wu AM, Hörnblad E, Voxeur A, Gerber L, Rihouey C, Lerouge P, Marchant A. 2010. Analysis of the Arabidopsis IRX9/IRX9-L and IRX14/IRX14-L pairs of glycosyltransferase genes reveals critical contributions to biosynthesis of the hemicellulose glucuronoxylan. Plant Physiology **153**, 542–554.

Wu AM, Rihouey C, Seveno M, Hörnblad E, Singh SK, Matsunaga T, Ishii T, Lerouge P, Marchant A. 2009. The Arabidopsis IRX10 and IRX10-LIKE glycosyltransferases are critical for glucuronoxylan biosynthesis during secondary cell wall formation. The Plant Journal **57**, 718–371.

Wu Q, Zhang X, Peirats-Llobet M, Belda-Palazon B, Wang X, Cui S, Yu X, Rodriguez PL, An C. 2016. Ubiquitin ligases RGLG1 and RGLG5 regulate abscisic acid signaling by controlling the turnover of phosphatase PP2CA. The Plant Cell **28**, 2178–2196.

Xie B, Wang X, Zhu M, Zhang Z, Hong Z. 2011. *Cals7* encodes a callose synthase responsible for callose deposition in the phloem. The Plant Journal **65**, 1–14.

Xie M, Zhang J, Yao T, ***et al.*** 2020. Arabidopsis C-terminal binding protein ANGUSTIFOLIA modulates transcriptional co-regulation of *MYB46* and *WRKY33*. New Phytologist **228**, 1627–1639.

Yue ZL, Liu N, Deng ZP, Zhang Y, Wu ZM, Zhao JL, Sun Y, Wang ZY, Zhang SW. 2022. The receptor kinase OsWAK11 monitors cell wall pectin changes to fine-tune brassinosteroid signaling and regulate cell elongation in rice. Current Biology **32**, 2454–2466.e7.

Zhang H, Wang Q, Blanco-Touriñán N, Hardtke CS. 2024. Antagonistic CLE peptide pathways shape root meristem tissue patterning. Nature Plants **10**, 1900–1908.

Zhang Y, Yin B, Zhang J, ***et al.*** 2019. Histone deacetylase HDT1 is involved in stem vascular development in Arabidopsis. International Journal of Molecular Sciences **20**, 3452.

Zhao Y, Song D, Sun J, Li L. 2013. *Populus* endo-beta-mannanase PtrMAN6 plays a role in coordinating cell wall remodeling with suppression of secondary wall thickening through generation of oligosaccharide signals. The Plant Journal **74**, 473–485.